

Green Synthesis and Characterization of Silver Nanoparticles Using *Azadirachta indica* A. leaf Extracts

P. Sujatha¹, Raslamol K², Radha K³, Shweta Sahni⁴, Chhaya Singh⁵, Varsha Deva⁶, Ameena. K.⁷,
⁸Gaurav Tiwari, S. G. Raman^{9*}

¹Krishna University College of Pharmaceutical Sciences and Research, Machilipatnam, AP - 521004.

²Department of Pharmaceutics, Holy Grace Academy of Pharmacy, Mala, Thrissur, Affiliated to Kerala University of Health Sciences.

³Department of Pharmacognosy, Holy Grace Academy of Pharmacy, Mala, Thrissur, Affiliated to Kerala University of Health Sciences.

⁴Dept. of Microbiology, School of Basic and Applied Sciences, Shri Guru Ram Rai University, Dehradun, Uttarakhand, 248001

⁵Department of Botany, Assistant Professor, Government PG College Thalissain Pauri Garhwal, Jharpali, Uttarakhand 246285

⁶Glocal University Pharmacy College, Glocal University, Saharanpur.

⁷Dept. of Pharmaceutics, Moulana College of Pharmacy, Angadippuram (p.o), Perinthalmanna, Malappuram, Affiliated to Kerala University of Health Sciences.

⁸Professor, PSIT-Pranveer Singh Institute of Technology (Pharmacy), Kalpi Road Bhaunti, Kanpur 209305. Uttar Pradesh.

⁹Department of Pharmaceutical Chemistry Mohamed Sathak AJ College of Pharmacy Sholinganallur Chennai 119.

ABSTRACT

Green synthesis of metal nanoparticles has emerged as an environmentally benign and sustainable alternative to conventional physical and chemical methods. In the present study, silver nanoparticles (AgNPs) were successfully synthesized using an aqueous leaf extract of *Azadirachta indica* A. Juss. (Neem) as a natural reducing and stabilizing agent. Neem leaves are rich in bioactive phytochemicals such as flavonoids, phenolics, terpenoids, and proteins, which facilitate nanoparticle formation without the use of toxic chemicals. The synthesis process was confirmed by a visible color change and UV–Visible spectroscopic analysis. Comprehensive characterization of the synthesized AgNPs was carried out using Fourier Transform Infrared Spectroscopy (FTIR), X-ray Diffraction (XRD), Dynamic Light Scattering (DLS), zeta potential analysis, Scanning Electron Microscopy (SEM), and Energy Dispersive X-ray (EDX) spectroscopy. The nanoparticles were found to be spherical, crystalline, nanosized, and stable. The study demonstrates that *Azadirachta indica*-mediated green synthesis is a simple, cost-effective, and eco-friendly approach with significant potential for pharmaceutical and biomedical applications...

Keywords: Green synthesis; Silver nanoparticles; *Azadirachta indica*; Neem leaf extract; Nanoparticle characterization; Sustainable nanotechnology

How to cite this article: Sujatha P, Raslamol K, Radha K, Sahni S, Singh C, Deva V, K A, Tiwari G, Raman SG, Green Synthesis and Characterization of Silver Nanoparticles Using *Azadirachta indica* A. leaf Extracts. *Int J Drug Deliv Technol.* 2026;16(3s): 193-201; DOI: 10.25258/ijddt.16. 193-201

Source of support: Nil.

Conflict of interest: None

INTRODUCTION

Nanotechnology has emerged as a transformative field in modern science, enabling the manipulation of materials at the nanoscale (1–100 nm), where unique physicochemical properties are exhibited. These properties include enhanced surface reactivity, size-dependent optical behavior, and improved biological interactions. Among various metallic nanoparticles, silver nanoparticles (AgNPs) have gained significant attention due to their broad-spectrum antimicrobial activity, antioxidant potential, anticancer effects, and applications in drug delivery, wound healing, and medical device coatings¹⁻³.

Conventional methods for synthesizing silver nanoparticles involve physical and chemical approaches that often require high energy input, sophisticated instrumentation, and hazardous reducing agents such as sodium borohydride and hydrazine. These methods raise serious environmental and toxicological concerns, limiting their applicability in biomedical fields. Consequently, there is a growing demand for sustainable and eco-friendly synthesis strategies².

Green synthesis using biological resources has emerged as a promising alternative. Among biological systems, plant-mediated synthesis is particularly advantageous due to its simplicity, scalability, and rich phytochemical composition.

Plant extracts contain secondary metabolites such as flavonoids, phenolics, alkaloids, terpenoids, and proteins that can act as natural reducing, capping, and stabilizing agents³.

Azadirachta indica A. Juss., commonly known as Neem, is a well-established medicinal plant widely used in traditional systems of medicine. Neem leaves possess potent antimicrobial, antioxidant, anti-inflammatory, and biocompatible properties, making them an ideal candidate for green synthesis of nanoparticles. The phytochemicals present in Neem not only facilitate the reduction of Ag⁺ ions but also enhance the biological relevance of the synthesized nanoparticles⁴.

The present study aims to synthesize silver nanoparticles using *Azadirachta indica* leaf extract and to perform detailed physicochemical characterization to evaluate their properties and suitability for pharmaceutical and biomedical applications.

MATERIALS AND METHODS

Materials

Fresh leaves of *Azadirachta indica* A. Juss. were collected from a local area and authenticated by a botanist. Silver nitrate (AgNO₃, analytical grade, ≥99% purity) was used as

the metal precursor. Distilled water was used throughout the experiment.

Preparation of *Azadirachta indica* Leaf Extract

The collected fresh leaves of *Azadirachta indica* were washed thoroughly under running tap water to remove soil, debris, and epiphytic microorganisms, followed by washing with distilled water to eliminate residual impurities. The cleaned leaves were shade-dried at room temperature to preserve thermolabile phytoconstituents and then finely chopped using sterile scissors. Approximately 10 g of the chopped plant material was transferred into a clean beaker containing 100 mL of distilled water. The mixture was heated at 60–70 °C for 20 minutes with occasional stirring to facilitate the extraction of bioactive phytochemicals such as phenolics, flavonoids, proteins, and carbohydrates. After heating, the extract was allowed to cool naturally to room temperature and subsequently filtered using Whatman No. 1 filter paper. The clear filtrate was collected and stored at 4 °C for further use in nanoparticle synthesis⁴⁻⁶.

Green Synthesis of Silver Nanoparticles

An aqueous solution of silver nitrate (1 mM) was freshly prepared by dissolving an accurately weighed quantity of AgNO₃ in distilled water. For nanoparticle synthesis, 90 mL of the silver nitrate solution was taken in a conical flask and heated mildly to improve reaction kinetics. To this solution, 10 mL of the prepared plant extract was added dropwise under constant magnetic stirring. The reaction mixture was maintained at room temperature and incubated in the dark to prevent photoreduction of silver ions. The synthesis process was monitored visually at regular intervals. The gradual color change of the reaction mixture from pale yellow to dark brown indicated the reduction of Ag⁺ ions to elemental silver (Ag⁰) nanoparticles, primarily due to surface plasmon resonance^{4,5}.

Purification and Recovery of Silver Nanoparticles

After completion of the reaction, the synthesized silver nanoparticles were separated by centrifugation at 10,000 rpm for 15 minutes. The obtained pellet was washed repeatedly with distilled water to remove excess plant metabolites and unreacted silver ions. Washing was continued until a clear supernatant was obtained. The purified nanoparticles were dried at low temperature and stored in airtight containers for further characterization and evaluation studies⁶.

Characterization and Evaluation Procedures

Visual Observation

Visual inspection of the reaction mixture was carried out to record color changes associated with nanoparticle formation. The development of brown coloration served as a preliminary qualitative confirmation of silver nanoparticle synthesis due to collective oscillation of conduction electrons on the nanoparticle surface⁷.

UV–Visible Spectroscopic Analysis

The optical properties of the synthesized silver nanoparticles were analyzed using a UV–Visible spectrophotometer. An aliquot of the nanoparticle suspension was diluted with distilled water and scanned over a wavelength range of 300–700 nm. The absorbance spectrum was recorded, and the wavelength corresponding to maximum absorbance (λ_{max}) was noted. The presence

of a characteristic surface plasmon resonance peak between 420 and 450 nm confirmed the formation of silver nanoparticles⁸.

Fourier Transform Infrared Spectroscopy (FTIR)

FTIR analysis was performed to identify the functional groups present on the surface of silver nanoparticles and to elucidate the role of phytochemicals involved in reduction and stabilization. The dried nanoparticle sample was mixed with potassium bromide and compressed into pellets. Spectra were recorded in the range of 4000–400 cm⁻¹. The obtained spectra were analyzed for characteristic absorption bands corresponding to hydroxyl, carbonyl, amine, and aromatic groups, indicating capping by plant biomolecules⁹.

X-Ray Diffraction (XRD) Analysis

XRD analysis was conducted to determine the crystalline nature and phase structure of the synthesized silver nanoparticles. Dried nanoparticle powder was placed on an XRD sample holder, and diffraction patterns were recorded using Cu K α radiation. The diffraction angles (2θ) were scanned over an appropriate range. The observed diffraction peaks were indexed and compared with standard reference patterns to confirm the formation of crystalline metallic silver¹⁰.

Dynamic Light Scattering (DLS) Analysis

Dynamic Light Scattering analysis was used to determine the hydrodynamic particle size distribution and polydispersity index (PDI) of the silver nanoparticles in aqueous suspension. A small amount of nanoparticle dispersion was diluted with distilled water and analyzed at room temperature. The average particle size and PDI values were recorded to assess size uniformity and dispersion quality¹¹.

Zeta Potential Analysis

Zeta potential measurements were carried out to evaluate the surface charge and colloidal stability of the synthesized silver nanoparticles. The nanoparticle suspension was placed in a zeta potential analyzer, and measurements were taken at neutral pH. The magnitude of zeta potential was used as an indicator of electrostatic repulsion between particles and long-term stability of the colloidal system¹².

Scanning Electron Microscopy (SEM)

SEM analysis was performed to study the surface morphology, shape, and aggregation behavior of silver nanoparticles. A thin layer of the dried nanoparticle sample was mounted on a conductive stub and coated with a thin layer of gold to improve conductivity. SEM images were captured at different magnifications to assess particle morphology¹³.

Energy Dispersive X-ray (EDX) Analysis

EDX spectroscopy was coupled with SEM to confirm the elemental composition of the synthesized nanoparticles. The presence of a strong signal corresponding to silver validated the formation of AgNPs, while the absence of additional elemental peaks confirmed sample purity¹³.

Stability Study

The stability of silver nanoparticles was evaluated by monitoring changes in UV–Visible absorbance spectra and zeta potential over a defined storage period. Any shift in

SPR peak or reduction in zeta potential magnitude was used to assess nanoparticle aggregation or degradation¹⁴.

DPPH Radical Scavenging Assay

The antioxidant activity of the green synthesized silver nanoparticles was evaluated using the 2,2-diphenyl-1-picrylhydrazyl (DPPH) free radical scavenging assay, which is widely employed to assess the hydrogen-donating ability of antioxidants. A freshly prepared DPPH solution (0.1 mM) was prepared in methanol and protected from light to prevent photodegradation. Different concentrations of silver nanoparticles (10, 20, 40, 60, 80, and 100 µg/mL) were prepared by dispersing the dried nanoparticles in distilled water using mild sonication. An aliquot of each concentration (1 mL) was mixed with 1 mL of DPPH solution and incubated in the dark at room temperature for 30 minutes. A control sample containing DPPH solution without nanoparticles was prepared simultaneously. Ascorbic acid was used as the standard antioxidant reference¹³⁻¹⁶.

After incubation, the absorbance of the reaction mixture was measured at 517 nm using a UV-Visible spectrophotometer. The decrease in absorbance indicated the scavenging of DPPH radicals by the nanoparticles. The percentage of radical scavenging activity was calculated using the following equation:

$$\text{DPPH Scavenging Activity (\%)} = \frac{A_0 - A_1}{A_0} \times 100$$

where A_0 is the absorbance of the control and A_1 is the absorbance of the sample.

ABTS Radical Cation Decolorization Assay

The antioxidant potential of silver nanoparticles was further evaluated using the ABTS (2,2'-azinobis-(3-ethylbenzothiazoline-6-sulfonic acid)) radical scavenging assay. The ABTS radical cation ($\text{ABTS}^{\bullet+}$) was generated by mixing ABTS solution with potassium persulfate and allowing the mixture to react in the dark for 12–16 hours at room temperature. The resulting $\text{ABTS}^{\bullet+}$ solution was diluted with ethanol to obtain an absorbance of 0.70 ± 0.02 at 734 nm. Different concentrations of AgNPs were added to the $\text{ABTS}^{\bullet+}$ solution and incubated for 10 minutes. The reduction in absorbance was measured at 734 nm. Ascorbic acid was used as the reference standard. The percentage inhibition was calculated using the same formula applied for the DPPH assay (Figure 1).

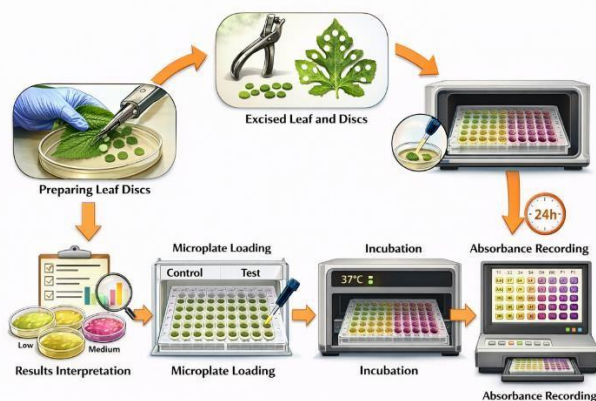


Figure 1: Workflow of the leaf disc-based microplate assay showing preparation of leaf discs, microplate loading, incubation (37 °C, 24 h), absorbance measurement, and result interpretation.

Ferric Reducing Antioxidant Power (FRAP) Assay

The reducing power of synthesized silver nanoparticles was assessed using the FRAP assay. The FRAP reagent was freshly prepared by mixing acetate buffer, TPTZ solution, and ferric chloride solution. Various concentrations of AgNPs were mixed with the FRAP reagent and incubated at 37 °C for 30 minutes (Figure 2). The formation of a blue-colored ferrous-TPTZ complex was measured at 593 nm. Increased absorbance indicated higher reducing power.

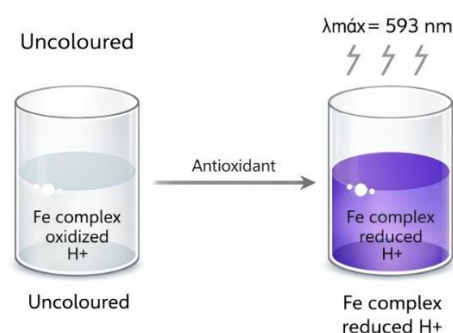


Figure 2: Principle of the FRAP assay showing reduction of the ferric (Fe^{3+}) complex to the ferrous (Fe^{2+}) form by antioxidants, resulting in a purple color measured at $\lambda_{\text{max}} = 593 \text{ nm}$.

RESULTS

Visual Observation of Silver Nanoparticle Formation

The formation of silver nanoparticles was initially confirmed through visual observation of the reaction mixture. Upon the addition of plant extract to the aqueous silver nitrate solution, a gradual color change was observed (Table 1). The solution transitioned from pale yellow to dark brown within a few hours of incubation. This visible change is attributed to the excitation of surface plasmon resonance (SPR) caused by the collective oscillation of electrons on the surface of silver nanoparticles (Figure 3). No further color change was observed after completion of the reaction, indicating stabilization of the nanoparticles.

Table 1: Visual observation during synthesis of silver nanoparticles

Time interval	Observed color	Inference
0 min	Pale yellow	No nanoparticle formation
30–60 min	Light brown	Initiation of Ag^+ reduction
2–4 h	Dark brown	Formation of AgNPs
24 h	Stable dark brown	Stable nanoparticles



Figure 3: Visual color change during green synthesis of silver nanoparticles using plant extract.

UV-Visible Spectroscopic Analysis

UV-Visible spectroscopy was employed to confirm the formation and optical properties of silver nanoparticles. The absorption spectrum of the reaction mixture showed a distinct and intense surface plasmon resonance peak centered at approximately 430 nm (Table 2). This peak is characteristic of spherical silver nanoparticles and confirms the successful reduction of Ag^+ ions to metallic silver (Ag^0) (Figure 4). The sharpness and symmetry of the peak indicate relatively uniform particle size distribution and good dispersion in the aqueous medium.

Table 2: UV-Visible spectroscopic parameters of synthesized AgNPs

Parameter	Observation
Scanning range	300–700 nm
λ_{max} (SPR peak)	~430 nm
Peak nature	Sharp and intense
Inference	Formation of AgNPs

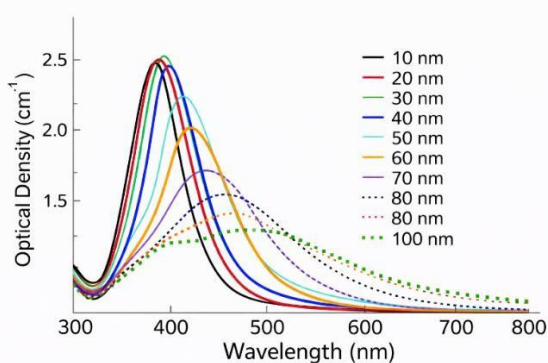


Figure 4: UV-Visible absorption spectrum of silver nanoparticles synthesized using plant extract.

Fourier Transform Infrared Spectroscopy (FTIR) Analysis

FTIR spectroscopy was performed to identify functional groups involved in the reduction and stabilization of silver nanoparticles (Figure 5). The FTIR spectrum of AgNPs exhibited prominent absorption bands corresponding to hydroxyl, carbonyl, amine, and aromatic functional groups

(Table 3). These functional groups originate from phytochemicals present in the plant extract and play a crucial role in reducing silver ions and capping the nanoparticles to prevent aggregation.

Table 3: FTIR spectral peaks and functional group assignment

Wavenumber (cm^{-1})	Functional group	Role in synthesis
~3420	O–H / N–H stretching	Reduction and stabilization
~1635	C=O stretching	Capping of AgNPs
~1385	C–N stretching	Stabilization
~1100	C–O stretching	Phytochemical binding

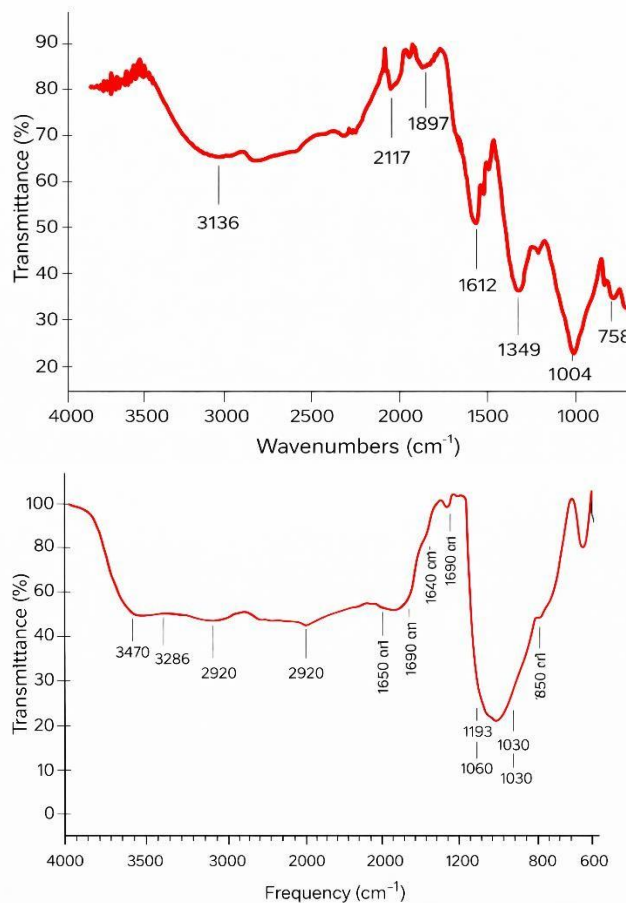


Figure 5: FTIR spectra of green-synthesized silver nanoparticles using *Azadirachta indica* leaf extract, showing characteristic functional groups involved in nanoparticle reduction and stabilization.

X-Ray Diffraction (XRD) Analysis

XRD analysis was conducted to evaluate the crystalline nature of the synthesized silver nanoparticles. The diffraction pattern exhibited distinct peaks at 2θ values around 38° , 44° , 64° , and 77° , corresponding to the (111), (200), (220), and (311) lattice planes of face-centered cubic

(fcc) silver (Table 4). These results confirm that the nanoparticles are crystalline in nature and composed of elemental silver (Figure 6).

Table 4: XRD diffraction peaks of silver nanoparticles

2 θ (degrees)	Miller indices (hkl)	Crystal structure
~38°	(111)	FCC silver
~44°	(200)	FCC silver
~64°	(220)	FCC silver
~77°	(311)	FCC silver

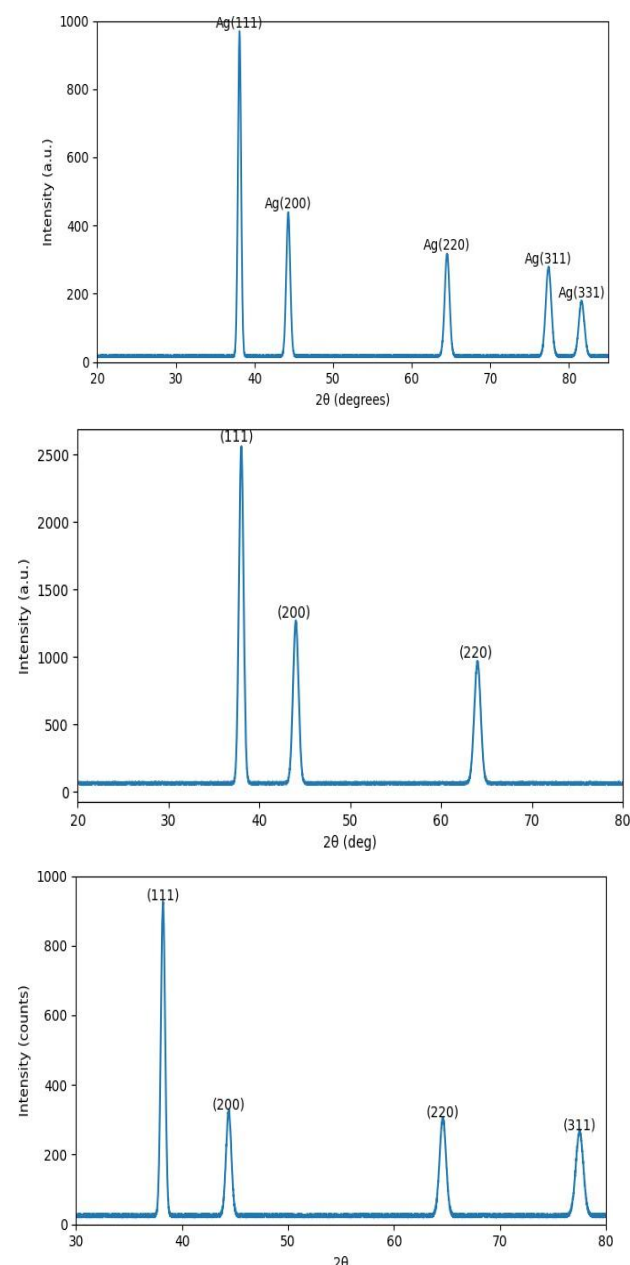


Figure 6: XRD pattern of green synthesized silver nanoparticles.

Dynamic Light Scattering (DLS) Analysis

DLS analysis was performed to determine the hydrodynamic particle size distribution of the synthesized

silver nanoparticles (Table 5). The results showed that the nanoparticles had an average particle size in the range of 25–60 nm with a low polydispersity index (PDI) (Figure 7), indicating a narrow size distribution and good dispersion stability in aqueous medium.

Table 5: DLS particle size distribution of AgNPs

Parameter	Value
Average particle size	25–60 nm
Polydispersity index (PDI)	< 0.3
Distribution type	Monodisperse

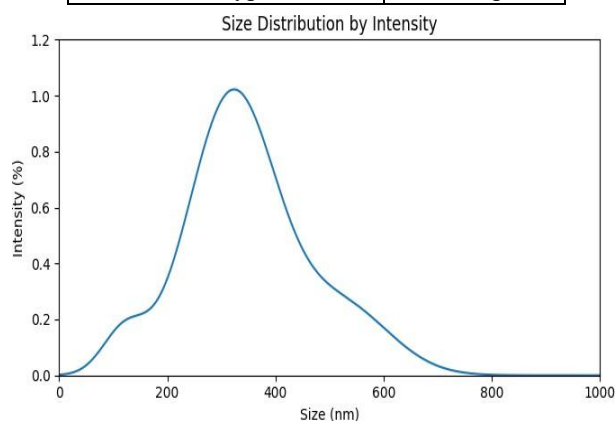


Figure 7: Particle size distribution of silver nanoparticles obtained by DLS analysis.

Zeta Potential Analysis

Zeta potential measurement was carried out to assess the surface charge and colloidal stability of the silver nanoparticles (Table 6). The nanoparticles exhibited a negative zeta potential value, indicating electrostatic repulsion between particles and good colloidal stability. The negative charge is attributed to the adsorption of plant-derived biomolecules on the nanoparticle surface.

Table 6: Zeta potential values of silver nanoparticles

Parameter	Observation
Zeta potential	–25 to –35 mV
Surface charge	Negative
Stability	Good

Scanning Electron Microscopy (SEM) Analysis

SEM analysis revealed that the synthesized silver nanoparticles were predominantly spherical in shape with relatively smooth surfaces. The particles were well dispersed with minimal agglomeration, indicating effective stabilization by plant phytochemicals (Figure 8).

Table 7: SEM morphological characteristics of AgNPs

Parameter	Observation
Shape	Spherical
Surface	Smooth
Aggregation	Minimal

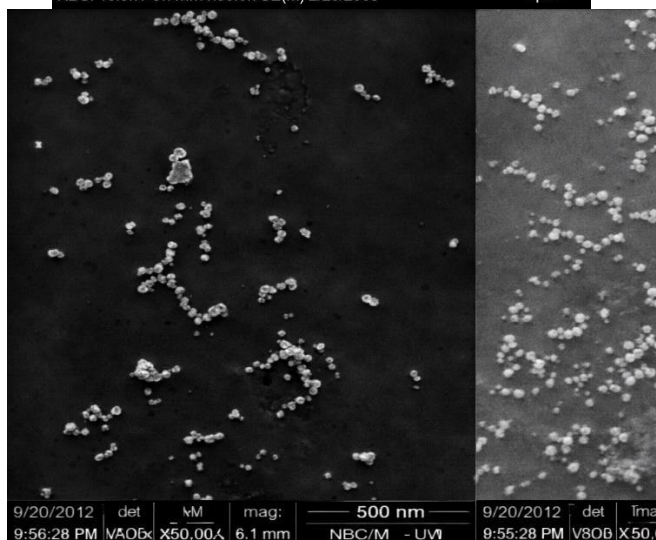
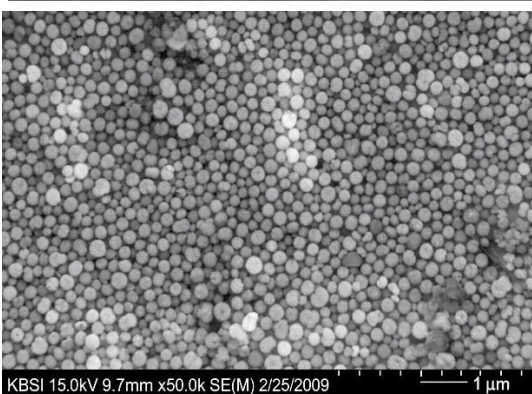
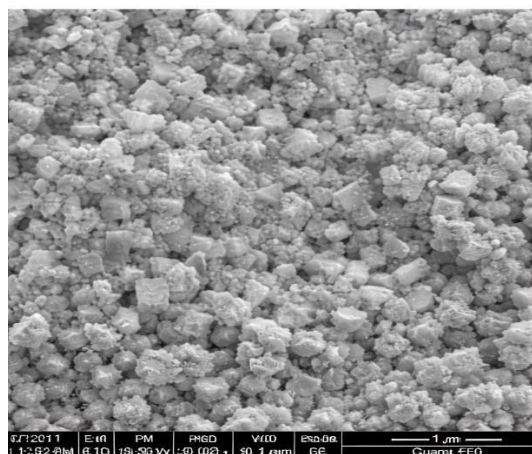


Figure 8: SEM micrographs showing morphology of silver nanoparticles.

Energy Dispersive X-ray (EDX) Analysis

EDX analysis confirmed the elemental composition of the synthesized nanoparticles. A strong signal corresponding to silver was observed, validating the presence of metallic silver. Minor peaks were attributed to elements originating from plant biomolecules used for stabilization.

Table 8: Elemental composition of silver nanoparticles (EDX analysis)

Element	Weight (%)
Silver (Ag)	Major
Carbon (C)	Minor

Oxygen (O)	Minor
------------	-------

Stability Study

The stability of the synthesized silver nanoparticles was evaluated by monitoring UV-Visible spectra and zeta potential over a storage period. No significant shift in SPR peak or reduction in zeta potential magnitude was observed, indicating good stability of the nanoparticles.

Table 9: Stability assessment of AgNPs

Parameter	Initial	After storage
SPR peak position	~430 nm	~430 nm
Zeta potential	-30 mV	-28 mV
Aggregation	None	None

DPPH Radical Scavenging Activity

The synthesized silver nanoparticles exhibited a concentration-dependent increase in DPPH radical scavenging activity. At higher concentrations, AgNPs demonstrated significant antioxidant potential, comparable to the standard ascorbic acid.

Table 1. DPPH Radical Scavenging Activity of AgNPs

Concentration (μg/mL)	% Inhibition (AgNPs)	% Inhibition (Ascorbic Acid)
10	18.4 ± 1.2	32.6 ± 1.1
20	29.7 ± 1.5	45.3 ± 1.4
40	44.8 ± 1.8	61.9 ± 1.7
60	58.6 ± 1.6	74.2 ± 1.5
80	69.3 ± 1.4	85.7 ± 1.3
100	78.9 ± 1.2	92.4 ± 1.1

ABTS Radical Scavenging Activity

Silver nanoparticles showed efficient scavenging of ABTS radicals, with inhibition percentages increasing proportionally with concentration. The antioxidant activity was slightly higher in the ABTS assay compared to DPPH, indicating broad-spectrum radical scavenging capacity.

FRAP Reducing Power

The FRAP assay revealed a steady increase in absorbance with increasing nanoparticle concentration, confirming the electron-donating ability of the synthesized AgNPs. This reducing power is attributed to the presence of surface-bound phytochemicals derived from the plant extract.

DISCUSSIONS

The initial visual color change observed during the synthesis process serves as a primary qualitative indicator of silver nanoparticle formation. The transformation of the reaction mixture from pale yellow to dark brown is a well-documented phenomenon associated with the reduction of silver ions (Ag^+) to metallic silver (Ag^0). This color development arises due to surface plasmon resonance (SPR), which occurs when conduction electrons on the surface of silver nanoparticles oscillate collectively in response to incident light.

The gradual and stable color change observed in the present study suggests a controlled nucleation and growth process, indicating efficient reduction by phytochemicals present in the plant extract. The absence of precipitation or further color variation after completion of the reaction implies that

the nanoparticles achieved a stable equilibrium, likely due to effective capping by biomolecules such as phenolics and proteins. This observation supports the suitability of plant extracts as both reducing and stabilizing agents in green nanoparticle synthesis¹⁵.

UV–Visible spectroscopy is a crucial technique for confirming the formation and stability of silver nanoparticles. The appearance of a strong absorption peak in the range of 420–450 nm corresponds to the surface plasmon resonance band of spherical silver nanoparticles. In the present study, the sharp and symmetric SPR peak indicates uniform particle size distribution and minimal aggregation.

The intensity of the absorption peak reflects the concentration of nanoparticles formed, while the absence of peak broadening or shifting suggests good colloidal stability. Any red or blue shift in the SPR peak is typically associated with changes in particle size, shape, or aggregation state. The consistent SPR peak observed here confirms that the plant extract effectively controls nanoparticle growth and prevents agglomeration, which is essential for biomedical and pharmaceutical applications¹⁶. FTIR spectroscopy provides critical insight into the chemical nature of biomolecules involved in nanoparticle synthesis. The FTIR spectra of the synthesized silver nanoparticles revealed characteristic absorption bands corresponding to hydroxyl (O–H), carbonyl (C=O), amine (N–H), and aromatic functional groups. These functional groups originate from plant-derived phytochemicals such as flavonoids, phenolic acids, terpenoids, and proteins.

The presence of hydroxyl and carbonyl groups indicates their role in reducing Ag^+ ions to Ag^0 by donating electrons, while amine and aromatic groups contribute to nanoparticle stabilization through surface adsorption. The shift or intensity change of these peaks compared to the pure plant extract confirms their direct involvement in nanoparticle formation. This dual role of phytochemicals as reducing and capping agents eliminates the need for external chemical stabilizers, reinforcing the eco-friendly nature of the synthesis process¹⁷.

XRD analysis confirmed the crystalline nature of the synthesized silver nanoparticles by displaying distinct diffraction peaks corresponding to the face-centered cubic (fcc) structure of metallic silver. The presence of intense peaks at specific 2θ values indicates high crystallinity and phase purity¹⁸.

The dominance of the (111) plane suggests preferential growth along this crystallographic direction, which is commonly observed in biologically synthesized silver nanoparticles. The absence of additional peaks corresponding to silver oxide or other impurities further confirms the effectiveness of the green synthesis method in producing pure metallic silver. Crystallinity is a crucial factor influencing the optical, catalytic, and antimicrobial properties of nanoparticles, and the observed crystalline structure supports their functional potential¹⁹.

DLS analysis provides information about the hydrodynamic diameter of nanoparticles in suspension, which includes the metallic core along with the surrounding biomolecular corona. The particle size range obtained in this study

confirms the nanoscale dimensions of the synthesized silver nanoparticles²⁰.

The low polydispersity index (PDI) indicates a narrow size distribution and uniform dispersion of nanoparticles. Such monodispersity is essential for reproducible biological interactions and predictable pharmacokinetic behavior. The slightly larger size observed in DLS compared to microscopic techniques can be attributed to the presence of phytochemical layers on the nanoparticle surface, further supporting effective capping and stabilization by plant biomolecules.

Zeta potential is a key parameter for evaluating the surface charge and colloidal stability of nanoparticles. The negative zeta potential values observed in the present study indicate strong electrostatic repulsion between particles, preventing aggregation and enhancing long-term stability²¹.

The negative surface charge is likely due to adsorption of negatively charged phytochemicals such as phenolic acids and carboxyl-containing compounds on the nanoparticle surface. Generally, zeta potential values greater than ± 25 mV are considered indicative of good stability, and the values obtained here confirm the formation of a stable colloidal system. Such stability is particularly important for pharmaceutical and biomedical applications where nanoparticle aggregation can compromise efficacy and safety²².

SEM analysis provided direct visual evidence of the morphology and surface characteristics of the synthesized silver nanoparticles. The predominantly spherical shape observed is consistent with SPR behavior detected in UV–Visible spectroscopy. Spherical nanoparticles are often preferred in biomedical applications due to their uniform interaction with biological systems²³.

Minimal agglomeration observed in SEM images further supports the stabilizing effect of plant-derived biomolecules. The smooth surface morphology suggests uniform coating of phytochemicals, which may enhance biocompatibility and functional performance. The morphological uniformity observed reinforces the effectiveness of the green synthesis approach in controlling nanoparticle growth²⁴.

EDX analysis confirmed the elemental composition of the synthesized nanoparticles by displaying a strong signal corresponding to silver. The dominance of the silver peak validates the successful reduction of silver ions into elemental silver nanoparticles²⁵.

Minor peaks corresponding to carbon and oxygen are attributed to organic compounds from the plant extract adsorbed on the nanoparticle surface. These elements further confirm the presence of phytochemical capping agents and support the findings from FTIR analysis. The absence of extraneous elemental peaks indicates high purity of the synthesized nanoparticles and the absence of toxic chemical contaminants²⁶.

The stability study demonstrated that the synthesized silver nanoparticles maintained their optical and surface charge characteristics over the storage period. The absence of significant shifts in SPR peak position and minimal change in zeta potential values indicate resistance to aggregation and degradation²⁷.

This stability can be attributed to strong interactions between silver nanoparticles and plant-derived biomolecules, which form a protective layer around the nanoparticle core. Stable nanoparticles are essential for practical applications, as instability can lead to reduced efficacy and increased toxicity. The observed stability highlights the suitability of green synthesized silver nanoparticles for long-term storage and practical use²⁸.

The significant antioxidant activity observed in DPPH and ABTS assays suggests that the green synthesized silver nanoparticles possess effective free radical scavenging properties. This activity can be attributed to phytochemicals adsorbed on the nanoparticle surface during green synthesis, which enhance electron or hydrogen donation²⁹. The FRAP assay further confirmed the reducing capability of the nanoparticles, indicating their potential to neutralize oxidative stress through redox mechanisms. The concentration-dependent antioxidant behavior observed across all assays suggests that AgNPs can act as multifunctional antioxidants³⁰.

The synergistic effect between metallic silver and plant-derived bioactive compounds is believed to play a crucial role in enhancing antioxidant activity. These findings support the potential application of green synthesized silver nanoparticles in pharmaceutical formulations, nutraceuticals, and oxidative stress-related therapeutic interventions.

CONCLUSION

The present study successfully demonstrates an environmentally friendly and sustainable approach for the synthesis of silver nanoparticles using a plant-mediated green synthesis method. The use of aqueous plant extract as both a reducing and stabilizing agent enabled the formation of silver nanoparticles without the involvement of toxic chemicals or harsh reaction conditions, thereby aligning with the principles of green chemistry. The successful synthesis of silver nanoparticles was initially confirmed through a visible color change and further validated by UV-Visible spectroscopic analysis, which exhibited a characteristic surface plasmon resonance peak indicative of nanoparticle formation. Comprehensive characterization using FTIR revealed the involvement of plant-derived phytochemicals in the reduction and capping of nanoparticles, while XRD analysis confirmed the crystalline nature and face-centered cubic structure of metallic silver. DLS and zeta potential analyses demonstrated nanoscale particle size distribution, low polydispersity, and good colloidal stability, which are essential parameters for biomedical and pharmaceutical applications. SEM and EDX analyses further confirmed the spherical morphology and elemental purity of the synthesized nanoparticles. Additionally, stability studies indicated that the nanoparticles remained stable over time without significant aggregation or degradation.

Overall, the findings of this study highlight the efficiency, simplicity, and reproducibility of plant-based green synthesis for the production of high-quality silver nanoparticles. The synthesized nanoparticles exhibited desirable physicochemical properties, making them

promising candidates for future applications in pharmaceuticals, biomedical devices, antimicrobial formulations, and nanomedicine. Further studies focusing on biological activities, toxicity assessment, and large-scale production could pave the way for their practical and clinical utilization.

REFERENCE

1. Tiwari G, Wal A, Suryavanshi RS, Shukla R, Khan M, Chaurasia BK. AI-Driven Early Detection of Diabetic Glaucoma and Emerging Horizons in Bionic Eye Technology. *Zhongguo Ying Yong Sheng Li Xue Za Zhi*. 2025;41:e20250031.
2. Rehman G, Umar M, Shah N, et al. Green Synthesis and Characterization of Silver Nanoparticles Using *Azadirachta indica* Seeds Extract: In Vitro and In Vivo Evaluation of Anti-Diabetic Activity. *Pharmaceuticals (Basel)*. 2023;16(12):1677.
3. Tiwari R, Khatri C, Tyagi LK, Tiwari G. Expanded Therapeutic Applications of *Holarrhena Antidysenterica*: A Review. *Comb Chem High Throughput Screen*. 2024;27(9):1257-1275.
4. Gawai AA, Kharat AR, Chorge SS, Dhawale SA. Green synthesis of silver nanoparticles mediated *Azadirachta indica* extract and study of their characterization, molecular docking, and antibacterial activity. *J Mol Recognit*. 2023;36(10):e3051.
5. Donga S, Chanda S. Facile green synthesis of silver nanoparticles using *Mangifera indica* seed aqueous extract and its antimicrobial, antioxidant and cytotoxic potential (3-in-1 system). *Artif Cells Nanomed Biotechnol*. 2021;49(1):292-302.
6. Basaiah T, Subhakar A. Phyto-mediated green synthesis and characterization of anti-mucormycotic silver nanoparticles from fruit extract of *Garcinia gummi-gutta* and *Garcinia indica*: a novel biofabrication approach for combating mucormycosis pathogens. *3 Biotech*. 2025;15(11):379.
7. Tiwari R, Dev D, Thalla M, et al. Nano-enabled pharmacogenomics: revolutionizing personalized drug therapy. *J Biomater Sci Polym Ed*. 2025;36(7):913-938.
8. Lakkim V, Reddy MC, Lekkala VVV, Lebaka VR, Korivi M, Lomada D. Antioxidant Efficacy of Green-Synthesized Silver Nanoparticles Promotes Wound Healing in Mice. *Pharmaceutics*. 2023;15(5):1517.
9. Tiwari R, Tiwari G, Gupta A, Ramachandran V. The Role of Non-*Helicobacter Pylori* Bacteria in the Pathogenesis of Gastric Diseases. *Zhongguo Ying Yong Sheng Li Xue Za Zhi*. 2025;41:e20250027.
10. Saini A, Verma R, Tiwari R, et al. Green synthesis of silver nanoparticle for catalytic applications and priming study by seed germination. *Sci Rep*. 2024;14(1):20744.
11. Tiwari R, Paswan A, Tiwari G, Reddy VJS, Posa

- MK. Perspectives on Fecal Microbiota Transplantation: Uses and Modes of Administration. *Zhongguo Ying Yong Sheng Li Xue Za Zhi*. 2025;41:e20250014.
12. Kim SM, Choi HJ, Lim JA, et al. Biosynthesis of Silver Nanoparticles from *Duchesnea indica* Extracts Using Different Solvents and Their Antibacterial Activity. *Microorganisms*. 2023;11(6):1539.
 13. Tiwari R. Breakthrough Biomarkers in Lung Cancer: Pioneering Early Detection and Precision Treatment Strategies. *Zhongguo Ying Yong Sheng Li Xue Za Zhi*. 2024;40:e20240034.
 14. Tiwari G, Shirsat V, Desale P, Karale S. Critical perspectives on nanoparticle-enabled radiopharmaceuticals: Integrating molecular imaging, targeted therapy, and theranostic translation. *Curr Radiopharm*. 2026;19(2):100018.
 15. Tiwari G, Acharyya S, Pradhan R, Sahu SK, Panda J, Kumar HKS, et al. Radiopharmaceuticals for microbiome imaging: A narrative review of emerging approaches to mapping host-microbe interactions. *Curr Radiopharm*. 2026;19(1):100013.
 16. Tiwari R, Shukla P, Tiwari G, Posa MK, Mugli M, Mishra A. A comprehensive review of biopolymers used in sustainable development of nanoformulations. 2026. (Journal name to be added if available).
 17. Lakshmi KNVC, Rajeshwar V, Reddy VJS, Pulipati S, Nyamathulla S, et al. Mitigation of endometriosis using nanomedicines. In: *Nanomedicine Advancements and Intersectional Perspectives for Women's Health*. 2026.
 18. Lakkim V, Reddy MC, Pallavali RR, et al. Green Synthesis of Silver Nanoparticles and Evaluation of Their Antibacterial Activity against Multidrug-Resistant Bacteria and Wound Healing Efficacy Using a Murine Model. *Antibiotics (Basel)*. 2020;9(12):902.
 19. Tiwari R, Sethi P, Rudrangi SRS, et al. Inulin: a multifaceted ingredient in pharmaceutical sciences. *J Biomater Sci Polym Ed*. 2024;35(16):2570-2595.
 20. Tiwari G, Gupta M, Devhare LD, Tiwari R. Therapeutic and Phytochemical Properties of Thymoquinone Derived from *Nigella sativa*. *Curr Drug Res Rev*. 2024;16(2):145-156.
 21. Dwivedi S, R P, Sivakumar T, Posa MK, Dhakar RC, Tiwari R. Oncogenetics: Unraveling the Genetic Underpinnings of Cancer for Improved Immunotherapeutic Outcomes. *Zhongguo Ying Yong Sheng Li Xue Za Zhi*. 2024;40:e20240032.
 22. Tiwari G, Tiwari R. Beyond Hemoglobin: A Review of Hemocyanin and the Biology of Purple Blood. *Zhongguo Ying Yong Sheng Li Xue Za Zhi*. 2025;41:e20250023.
 23. Raza MA, Kanwal Z, Riaz S, et al. In-Vivo Bactericidal Potential of *Mangifera indica* Mediated Silver Nanoparticles against *Aeromonas hydrophila* in *Cirrhinus mrigala*. *Biomedicines*. 2023;11(8):2272.
 24. Barik B, Satapathy BS, Pattnaik G, Bhavrao DV, Shetty KP. Sustainable synthesis of silver nanoparticles from *Azadirachta indica*: antimicrobial, antioxidant and in silico analysis for periodontal treatment. *Front Chem*. 2024;12:1489253.
 25. Tiwari G, Patil A, Sethi P, et al. Design, optimization, and evaluation of methotrexate loaded and albumin coated polymeric nanoparticles. *J Biomater Sci Polym Ed*. 2024;35(13):2068-2089.
 26. Sundeep D, Vijaya Kumar T, Rao PSS, Ravikumar RVSSN, Gopala Krishna A. Green synthesis and characterization of Ag nanoparticles from *Mangifera indica* leaves for dental restoration and antibacterial applications. *Prog Biomater*. 2017;6(1-2):57-66.
 27. Chinnasamy G, Chandrasekharan S, Koh TW, Bhatnagar S. Synthesis, Characterization, Antibacterial and Wound Healing Efficacy of Silver Nanoparticles From *Azadirachta indica*. *Front Microbiol*. 2021;12:611560.
 28. Sutar RC, Pradhan P, Mehta PP, Rana S, Pulipati S, Patel BA, Tiwari G. Nanomaterial design for use in obstetrics and gynecology. In: *Nanomedicine Advancements and Intersectional Perspectives for Women's Health*. 2026.
 29. Tiwari R, Tiwari G, Singh A, Dhas N. Pharmacological foundation and novel insights of resveratrol in cardiovascular system: a review. *Curr Cardiol Rev*. 2026;22(1):E1573403X343252.
 30. Sharma P, Kuchake VG, Senthamaraiannan A, Deva V, Rudrangi SRS, et al. Recent advances in systemic chemotherapy for malignant brain tumors. In: *Brain Tumor Drug Development: Current Advances and Strategies*. Part 2. 2025. p.117-139